

# Postsynaptic CPG15 promotes synaptic maturation and presynaptic axon arbor elaboration *in vivo*

Isabel Cantallops, Kurt Haas and Hollis T. Cline

Cold Spring Harbor Laboratory, 1 Bungtown Rd., Cold Spring Harbor, New York 11724, USA

The first two authors contributed equally to this work

Correspondence should be addressed to H.T.C. ([cline@cshl.org](mailto:cline@cshl.org))

The formation of CNS circuits is characterized by the coordinated development of neuronal structure and synaptic function. The activity-regulated candidate plasticity gene 15 (*cpg15*) encodes a glycosylphosphatidylinositol (GPI)-linked protein whose *in vivo* expression increases the dendritic arbor growth rate of *Xenopus* optic tectal cells. We now demonstrate that tectal cell expression of CPG15 significantly increases the elaboration of presynaptic retinal axons by decreasing rates of branch retractions. Whole-cell recordings from optic tectal neurons indicate that CPG15 expression promotes retinotectal synapse maturation by recruiting functional AMPA receptors to synapses. Expression of truncated CPG15, lacking its GPI anchor, does not promote axon arbor growth and blocks synaptic maturation. These results suggest that CPG15 coordinately increases the growth of pre- and postsynaptic structures and the number and strength of their synaptic contacts.

Axonal and dendritic arbor structure and the distribution of synapses determine the connectivity between neurons, their integrative properties and their function within a neural circuit<sup>1-4</sup>. The elaboration of presynaptic axonal arbors and postsynaptic dendritic arbors and synaptogenesis occur simultaneously during brain development. Presynaptic axons and postsynaptic dendrites of target neurons attain reproducible arbor sizes and establish synapses with characteristic distributions and strengths<sup>3,4</sup>. The highly reproducible organization of the circuit suggests the existence of intercellular signaling mechanisms that coordinate these mechanisms.

We have examined the structural and functional development of the retinotectal projection in *Xenopus* to assess whether these features develop independently of one another *in vivo*. Developing glutamatergic synapses in the retinotectal projection of *Xenopus*<sup>5</sup>, as in other systems<sup>6-9</sup>, go through a maturation process in which newly formed synapses, mediated solely by the NMDA type of glutamate receptor, add AMPA receptors as they mature. Synapses with some AMPA receptors can mature further by the addition of more AMPA receptors. This maturation process occurs synapse by synapse, producing neurons with heterogeneous synaptic inputs with respect to the fraction of pure NMDA synapses and AMPA/NMDA ratios<sup>5,7,8</sup>. Consistent with these electrophysiological studies, quantitative immuno-electron microscopy has demonstrated the existence of synapses with only NMDA receptors in the brains of young rats and shown that the number of AMPA receptors increases at individual synapses as they mature<sup>10,11</sup>.

*In vivo* imaging studies show that optic tectal cell dendritic arbors undergo a period of rapid growth, followed by a slower growth phase<sup>12,13</sup>. Furthermore, dendritic arbors show rapid rates of branch additions and retractions during the period of rapid growth, and rates of dynamic branch rearrangements slow significantly during the slower growth phase, suggesting a correlation between branch dynamics and net arbor growth<sup>13</sup>. By

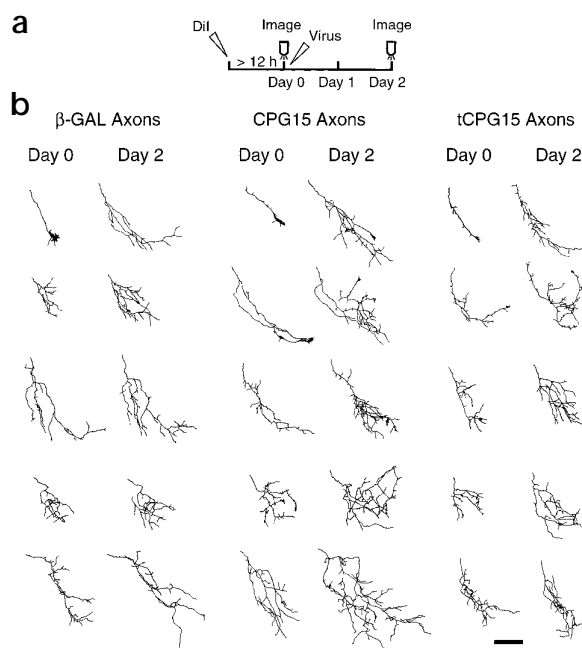
comparing the morphology and arbor dynamics of the tectal cells with their synaptic maturation, we find that dendritic arbors of neurons with low AMPA/NMDA ratios are more dynamic than arbors of neurons with high AMPA/NMDA ratios<sup>13,14</sup>. These data suggest that synapses with stronger synaptic transmission actively stabilize the branches bearing those synapses.

Experimental manipulation of CaMKII activity in optic tectal neurons provided further evidence for coordination of the development of synaptic strength and the growth rates of presynaptic axonal arbors and postsynaptic dendritic arbors. Increased postsynaptic CaMKII activity enhances the maturation of retinotectal synapses<sup>5</sup> and concomitantly slows the growth rates of both presynaptic axon and postsynaptic dendritic arbors<sup>12,15</sup>. Blocking endogenous tectal cell CaMKII enhances the dynamics and growth rates of both axons and dendrites<sup>12,16</sup>. The remarkable lock-step coordination of synaptic strength and neuronal arbor development could be most easily explained by the existence of activity-dependent intercellular signaling molecules that can coordinate presynaptic axon arbor development with postsynaptic dendritic arbors and the synaptic connections between them. Candidate molecules performing such a function have been identified from differential screens for genes induced by activity (reviewed in ref. 17).

The *cpg15* gene (also called *neurtin*<sup>18</sup>) was discovered in a differential screen for genes upregulated by activity in adult hippocampus<sup>19</sup>. Peak expression of *cpg15* occurs during periods of neuronal arbor growth and synaptogenesis<sup>20</sup>. CPG15 is a small, highly conserved<sup>18,21</sup> protein whose sequence predicts a secreted molecule that is attached to the extracellular membrane through a glycosylphosphatidylinositol (GPI) anchor<sup>18</sup>. Many GPI-linked proteins are involved in development of nervous system structure, likely because of their function in intercellular signaling pathways<sup>22,23</sup>.

CPG15 induces dramatic growth of dendritic arbors in a non-cell autonomous manner *in vivo*, consistent with the predicted cell-

**Fig. 1.** CPG15 expression in tectal neurons increases growth of presynaptic retinotectal axons. (a) Protocol for virus injection and axon imaging. (b) Drawings of representative retinal axon arbors collected before (day 0) and two days after (day 2) infection of optic tectal neurons with virus expressing  $\beta$ -gal, CPG15 or tCPG15. The five examples for each virus are arranged in rows by their similar morphology at day 0. Note the stronger growth-promoting effect of CPG15 on axons of larger complexity. Scale bar, 40  $\mu$ m.



surface location and a potential role in intercellular signaling<sup>24</sup>. The activity-dependent regulation of *cpg15* transcript<sup>19–21</sup> and protein<sup>24</sup>, together with the *cpg15*'s ability to enhance dendritic arbor development, suggest that it may function as an activity-dependent effector molecule that concomitantly regulates multiple aspects of circuit development. To test this hypothesis, we examined the effect of CPG15 expression on retinal ganglion cell axon arbor elaboration and retinotectal synaptic transmission. Our results demonstrate that postsynaptic expression of CPG15 enhances the elaboration of presynaptic retinal axon arbors and promotes the maturation of retinotectal synapses. Together with our previous studies showing that CPG15 enhances dendritic arbor elaboration<sup>24</sup>, these results support a model in which initial activity within a nascent circuit can induce activity-regulated genes, whose protein products in turn promote the coordinated development of the circuit.

## RESULTS

### CPG15 increases axonal growth rate

To test the potential role of CPG15 in regulating presynaptic axonal arbor structure, we imaged single Dil-labeled retinal ganglion cell (RGC) axons within the optic tectum of *Xenopus laevis* tadpoles. We infected their postsynaptic partners, the optic tectal cells, with vaccinia virus (VV) expressing the reporter  $\beta$ -galactosidase ( $\beta$ -gal-VV) or with virus expressing  $\beta$ -gal along with CPG15 (CPG15-VV). Retinal axon arbors from animals infected with  $\beta$ -gal-VV were identical to axons from uninfected control animals with respect to axonal growth rates and branch dynamics<sup>15</sup>, and were used as controls. We imaged the axons immediately before infection and two days later (Fig. 1a), when virally expressed protein is detectable in tectal cells<sup>24</sup>.

The initial images of retinotectal axons, collected before infection (day 0) showed a range of arbor complexities, from simple unbranched axons, terminating in a single growth cone, to highly branched arbors (Fig. 1b), as previously described<sup>15,25–27</sup>. A comparable range of arbor morphologies was seen at the initial time point in all experimental groups (Table 1).

Expression of CPG15 in optic tectal neurons significantly increased the growth rate of retinal axons over a two-day period

compared to axons from animals infected with  $\beta$ -gal-VV (Fig. 1b). The average growth rate of retinal axons from animals infected with  $\beta$ -gal-VV (called  $\beta$ -gal axons) was  $172 \pm 30.9 \mu$ m per 2 days (mean  $\pm$  s.e.m.,  $n = 34$ ). The average growth rate of retinal axons from animals infected with CPG15-VV (called CPG15 axons) was significantly greater, at  $255.6 \pm 39.9 \mu$ m per 2 days ( $n = 30$ ,  $p < 0.05$ ).

Studies have suggested that growth rates of retinal axons slow down as they become more complex<sup>5,27</sup>. Consistent with this, we found that complex control axons are structurally more stable than simple axons, which showed relatively large structural changes over two days. Furthermore, the effect of CPG15 on presynaptic RGC axonal arbor growth appeared more pronounced in complex axons (Fig. 2). We then quantitatively assessed whether simple and complex control axons have different growth rates over a two-day period, and whether CPG15 affects the two populations differently.

Scatterplots of growth rate versus initial axon arbor branch length showed that growth rates are greater for simple axons than more complex axons (Fig. 2). The growth rates of many simple axons fall above the mean growth rate of the entire population (horizontal bar at about 180  $\mu$ m in Fig. 2a), whereas the growth rates of few complex axons are above the mean. Simple  $\beta$ -gal axons, with initial total axon branch lengths (TABL) less than

**Table 1.** Morphometric parameters of retinal axons.

Treatment	Complexity	n	TABL ( $\mu$ m)			Branch number				
			day 0	day 2	$p^a$	day 0	day 2	$p^a$	day 2 – day 0	$p^b$
$\beta$ -gal	Simple	22	178.24 $\pm$ 14.18	385.82 $\pm$ 46.25	–	13.68 $\pm$ 1.86	25.50 $\pm$ 3.18	–	11.82 $\pm$ 2.95	–
	Complex	12	452.86 $\pm$ 29.02	559.52 $\pm$ 46.59	–	30.00 $\pm$ 1.61	34.50 $\pm$ 4.35	–	4.50 $\pm$ 4.30	–
CPG15	Simple	15	190.49 $\pm$ 17.20	478.60 $\pm$ 70.29	0.29	14.13 $\pm$ 2.45	27.80 $\pm$ 4.78	0.44	13.67 $\pm$ 3.44	0.33
	Complex	15	424.03 $\pm$ 22.54	647.19 $\pm$ 57.20	0.22	33.47 $\pm$ 2.61	40.33 $\pm$ 3.82	0.15	6.87 $\pm$ 4.58	0.35
tCPG15	Simple	32	166.00 $\pm$ 10.83	446.29 $\pm$ 37.12	0.25	12.50 $\pm$ 1.41	26.84 $\pm$ 2.75	0.30	14.34 $\pm$ 2.10	0.23
	Complex	12	408.00 $\pm$ 30.71	576.57 $\pm$ 38.55	0.15	27.08 $\pm$ 2.69	35.33 $\pm$ 3.55	0.18	8.25 $\pm$ 3.05	0.24

<sup>a</sup> Day 0 average compared with that of  $\beta$ -gal of same complexity, independent two-population *t*-test.

<sup>b</sup> Branch addition average compared with that of  $\beta$ -gal of same complexity, independent two-population *t*-test.

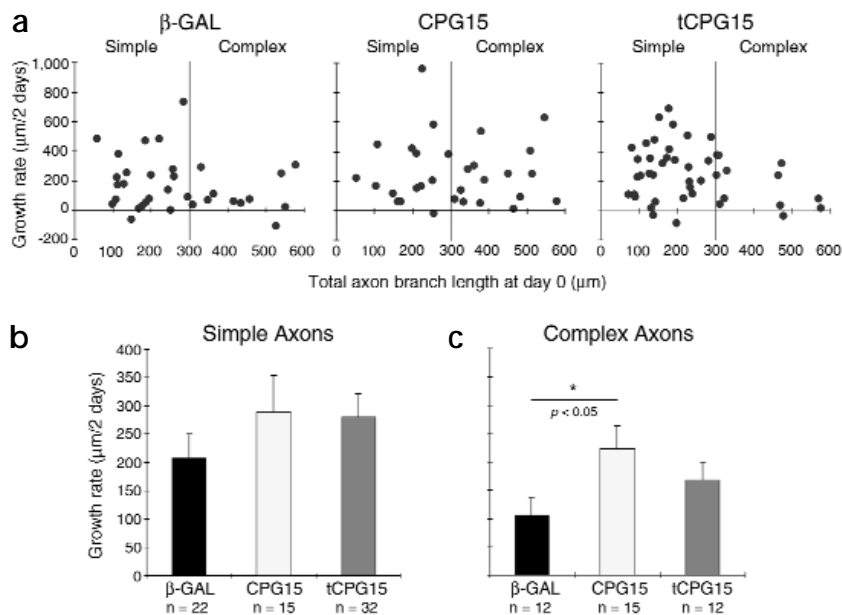


**Fig. 2.** Growth rates of complex axons are selectively affected by CPG15. (a) Scatterplots of axonal growth rate over two days versus total axon arbor branch length at day 0. Growth rates of simple axons, with initial branch length  $< 300 \mu\text{m}$ , are higher than complex axons, with initial branch length  $> 300 \mu\text{m}$ . A vertical line at  $300 \mu\text{m}$  along the x axis separates these two groups to ease comparison. A horizontal line at  $180 \mu\text{m}$  on the y axis marks the average growth rate of the entire population of the  $\beta$ -gal axons. CPG15 significantly increases the growth rate of complex axons. Note the higher proportion of complex CPG15 axons with growth rates above the horizontal line marking the average  $\beta$ -gal axon growth rate. The tCPG15 axons display a similar distribution to that of  $\beta$ -gal axons. Average growth rates for simple (b) and complex (c) axons from the three treatments. The numbers of axons analyzed are shown at the bottom of each bar.

$300 \mu\text{m}$  grow faster ( $207.6 \pm 39.2 \mu\text{m}$  per 2 days) than more complex  $\beta$ -gal axons with initial TABL greater than  $300 \mu\text{m}$  ( $106.7 \pm 35.0 \mu\text{m}$  per 2 days). The growth rate of simple CPG15 axons was not significantly different from that of simple  $\beta$ -gal axons ( $288.1 \pm 64.7 \mu\text{m}$  per 2 days). The growth rate of complex CPG15 axons, however, was significantly greater than that of complex  $\beta$ -gal axons ( $223.2 \pm 47.6 \mu\text{m}$  per 2 days, Fig. 2,  $p < 0.05$ ), and was comparable to the rapid growth rate of simple  $\beta$ -gal axons. We did not detect an effect of CPG15 expression on branch number over the two-day period (Table 1).

To test whether CPG15 must be bound to the cell surface to be biologically active, we expressed a truncated form of CPG15, lacking the GPI consensus sequence (tCPG15-VV). This construct produces a secreted soluble form of CPG15 (ref. 18). Retinal axon growth rates in animals expressing tCPG15 were not significantly different from those of  $\beta$ -gal axons (simple tCPG15 axons,  $279.9 \pm 34.1 \mu\text{m}$  per 2 days; complex tCPG15 axons,  $168.1 \pm 42.8 \mu\text{m}$  per 2 days; Figs. 1b and 2). No difference was observed in branch number over two days compared to control axons (Table 1).

In summary, postsynaptic expression of CPG15 increased the growth rate of presynaptic retinal axons, in a GPI-linkage-dependent manner.

### CPG15 enhances axon arbor dynamics

Retinal axon arbor elaboration occurs through the maintenance of a small fraction of newly added branches<sup>28</sup>. Increased arbor elaboration could result from a relative increase in rates of branch additions or a relative decrease in rates of branch retractions. To test whether CPG15 affects rates of branch additions or retractions, we collected images of single axons every two hours over eight hours starting two days after virus injection (Fig. 3a). This allowed us to follow the fate of every imaged branch in the arbor and determine rates of branch additions and retractions over the eight-hour period. Analysis was performed by dividing RGC axons into simple and complex groups, according to their TABL before infection.

Over eight hours, simple  $\beta$ -gal axons displayed a net arbor growth, whereas complex  $\beta$ -gal axons displayed a net decrease in axon arbor branch length due to selective pruning of fine branch tips (Fig. 3b). The branch dynamics of simple  $\beta$ -gal axons were

also significantly different from those of complex  $\beta$ -gal axons. Over the 8-hour period, simple axons displayed a net gain in branch number of  $11 \pm 7\%$ , whereas complex axons lost  $7 \pm 4\%$  of their branches ( $p < 0.05$ , Fig. 4a). Consistent with this result, simple axons retracted fewer branches than complex axons (simple,  $55 \pm 3\%$  per 8 h; complex,  $63 \pm 2\%$  per 8 h,  $p < 0.05$ ; Fig. 4b).

Postsynaptic expression of CPG15 increased the growth rate of complex axons to match that of the faster growing simple axons, as also seen over two days (Fig. 2). The relative change in branch number and the rate of branch retractions over eight hours in simple and complex CPG15 axons were comparable, in contrast to control  $\beta$ -gal axons, in which simple axons were more dynamic than complex axons. The enhanced growth rate of complex

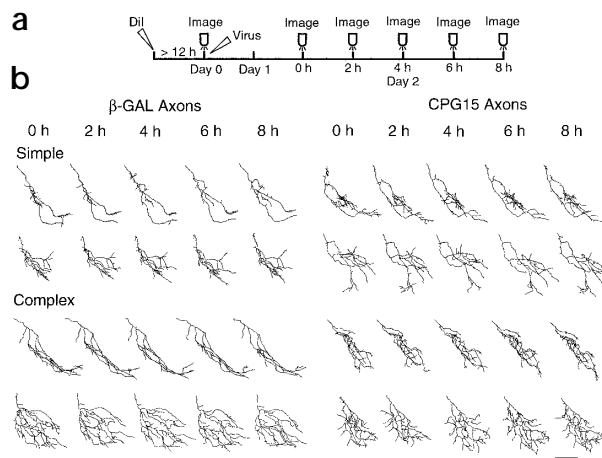


**Fig. 3.** CPG15 alters axon branch dynamics. (a) Protocol for virus injection and axon imaging. (b) Drawings of representative retinal axon arbors imaged every 2 h over 8 h from animals infected with either  $\beta$ -gal- or CPG15-VV. Simple  $\beta$ -gal and CPG15 axons display similar dynamics. Complex  $\beta$ -gal axons eliminate small branches over the observation interval (compare 0 h and 8 h), whereas complex CPG15 axons maintain them. Scale bar,  $40 \mu\text{m}$ .

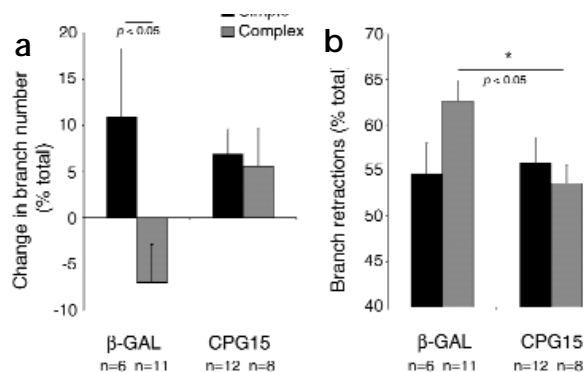


**Fig. 4.** CPG15 decreases rates of branch retractions in complex axons. Relative change in branch tip numbers (**a**) and branch retractions (**b**) in simple and complex axons from animals infected with  $\beta$ -gal- or CPG15-VV. Simple  $\beta$ -gal axons retract fewer branches than complex  $\beta$ -gal axons, resulting in a significant increase in branch numbers over 8 h. Complex CPG15 axons retract significantly fewer branches than complex  $\beta$ -gal axons. The numbers of axons analyzed are shown at the bottom of each bar.

CPG15 axons was due to a significant decrease in the rate of branch retractions (CPG15,  $54 \pm 2\%$  per 8 h;  $\beta$ -gal,  $63 \pm 2\%$  per 8 h; **Fig. 4b**,  $p < 0.05$ ), rather than an increase in branch additions (CPG15,  $60 \pm 3\%$  per 8 h;  $\beta$ -gal,  $56 \pm 3\%$  per 8 h).

#### CPG15 increases retinotectal synapse maturation

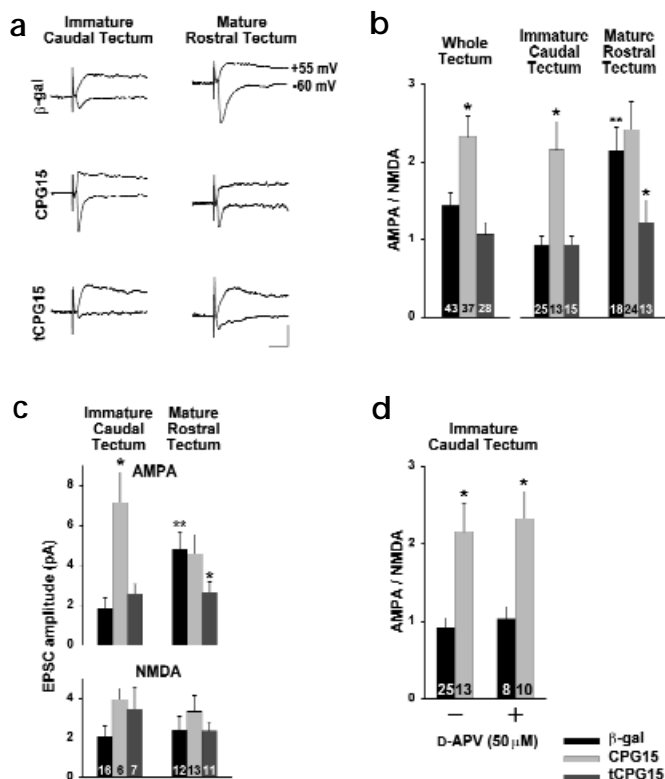
The growth-promoting effect of CPG15 on both presynaptic axons and postsynaptic dendrites suggests that CPG15 affects the synaptic connections between these partners. To test this, we made whole-cell voltage-clamp recordings from optic tectal neurons in animals

infected with  $\beta$ -gal-, CPG15- or tCPG15-VV. Glutamatergic retinotectal synaptic responses of neurons from animals infected with  $\beta$ -gal-VV are indistinguishable from those of neurons from uninfected animals<sup>5</sup> and were used as controls. We stimulated retinal axons in the optic chiasm to evoke monosynaptic excitatory postsynaptic currents (EPSCs) in tectal neurons, which are mediated by both AMPA and NMDA type glutamate receptors<sup>5,29,30</sup>.

Optic tectal neuronal cell bodies are organized along a rostrocaudal developmental gradient generated by a proliferative zone at the caudomedial edge of the tectum<sup>13,31</sup>. As tectal neurons are sampled at different positions along the rostrocaudal developmental axis, the relative contribution of AMPA receptors to the evoked synaptic current increases as neurons mature, whereas the amplitude of the NMDA component does not change (**Fig. 5a**). As described<sup>5</sup>, this causes a significant increase in the ratio of the amplitudes of the AMPA receptor and NMDA receptor-mediated currents (AMPA/NMDA ratio) in mature neurons in the rostral half of the tectum compared to immature neurons in the caudal half of the tectum (caudal neurons,  $0.9 \pm 0.1$ ; rostral neurons,  $2.2 \pm 0.03$ ,  $p < 0.001$ ; **Fig. 5b**). Importantly, there is no physical correlation between simple and complex axons and the location of immature and mature tectal neurons along the rostrocaudal gradient<sup>25,32</sup>. Simple axons can contact both mature and immature tectal neurons. Similarly, complex axons can contact both mature and immature tectal neurons.

CPG15 expression significantly increased the AMPA/NMDA ratio of evoked retinotectal synaptic responses averaged from all recorded neurons (CPG15,  $2.3 \pm 0.3$ ;  $\beta$ -gal,  $1.4 \pm 0.2$ ,  $p < 0.01$ ). To determine whether CPG15 expression selectively affected the strength of synaptic transmission in immature or mature neurons, we compared the AMPA/NMDA ratios of neurons in caudal tectum with those in rostral tectum. CPG15 expression significantly increased the AMPA/NMDA ratio of immature cau-

**Fig. 5.** CPG15 increases AMPA/NMDA ratios. (**a**) Evoked EPSCs recorded at  $V_h = +55$  mV (top traces) and  $V_h = -60$  mV (bottom traces) from brains infected with  $\beta$ -gal-, CPG15- and tCPG15-VV. Traces are averages of 50 to 100 responses. The relative contribution of the AMPA-receptor current increases with development. CPG15 expression increases the relative contribution of the AMPA-receptor-mediated current to the evoked responses in immature tectal neurons. tCPG15 reduces the AMPA-receptor-mediated component of the evoked response in mature tectal neurons. (**b**) AMPA/NMDA ratios of all tectal neurons recorded, or separately from neurons in caudal or rostral tectum. CPG15 significantly increased the AMPA/NMDA ratio in immature neurons, and tCPG15 significantly decreased AMPA/NMDA in mature neurons. (**c**) Amplitudes of synaptic currents evoked by minimal stimulation at  $V_h = -60$  mV (AMPA) and  $V_h = +55$  mV (NMDA). CPG15 increased the amplitude of AMPA-receptor-mediated currents in caudal cells. tCPG15 reduced the amplitude of AMPA-receptor-mediated currents in rostral cells. (**d**) NMDA receptor activity is not required for CPG15-induced increase in AMPA/NMDA ratio. Animals infected with  $\beta$ -gal- or CPG15-VV were treated with D-APV (right) or untreated (left). Legend in (**d**) applies to (**b**) and (**c**). The numbers of neurons analyzed are shown at the bottom of each bar. \*significant differences compared to relevant  $\beta$ -gal-VV controls,  $p < 0.05$ . \*\*significant differences between caudal and rostral neurons from animals infected with  $\beta$ -gal-VV,  $p < 0.05$ . Scale bar, 10 pA, 100 ms.



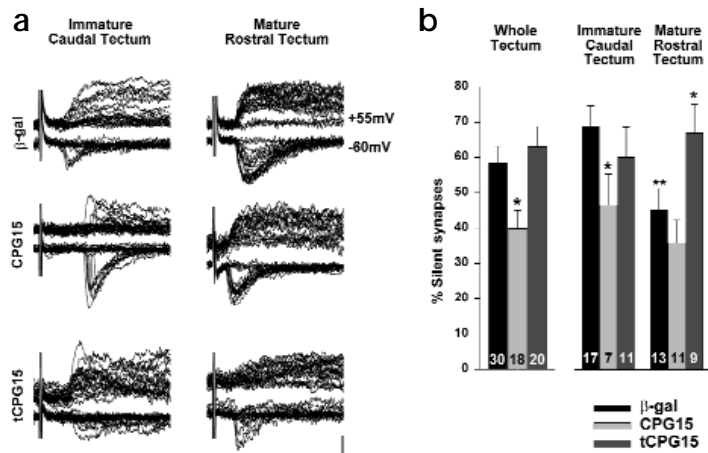


**Fig. 6.** CPG15 converts silent synapses to functional synapses. (a) Evoked responses from neurons in caudal or rostral tectum of animals infected with  $\beta$ -gal-, CPG15 or tCPG15-VV, recorded at  $V_h = +55$  mV (top traces) and  $V_h = -60$  mV (bottom traces). Overlays of 20 consecutive traces are shown. (b) Fraction of silent synapses in all tectal neurons recorded, or neurons from caudal or rostral tectum. CPG15 expression decreased the fraction of silent synapses in immature neurons. tCPG15 expression increased the fraction of silent synapses in mature neurons. The number of neurons recorded are shown at the bottom of each bar. \*significant differences compared to relevant  $\beta$ -gal-VV controls,  $p < 0.05$ . \*\*significant differences between caudal and rostral neurons from animals infected with  $\beta$ -gal-VV.  $p < 0.05$ . Horizontal scale bar, 10 ms. Vertical scale bar, 10 pA for rostral neurons from  $\beta$ -gal-VV and tCPG15-VV animals and 15 pA for all remaining panels.

dal neurons (CPG15,  $2.2 \pm 0.4$ ;  $\beta$ -gal,  $0.9 \pm 0.1$ ,  $p < 0.01$ ), resulting in neurons in immature regions of tectum with mature phenotypes of relatively large AMPA receptor contribution to evoked synaptic currents (Fig. 5a). CPG15 expression did not significantly affect the AMPA/NMDA ratios in mature neurons in rostral tectum (CPG15,  $2.4 \pm 0.4$ ;  $\beta$ -gal,  $2.2 \pm 0.3$ ).

The increase in AMPA/NMDA ratio may arise from an increase in AMPA-receptor-mediated currents or a decrease in NMDA-receptor-mediated-contribution to the EPSC. To test whether CPG15 selectively affected NMDA or AMPA receptor currents, we used a minimal stimulation protocol to excite single or a limited number of axons terminating on the recorded neuron<sup>5</sup>. CPG15 expression significantly increased the amplitude of AMPA-receptor-mediated currents in neurons from caudal tectum (CPG15,  $7.1 \pm 1.5$  pA;  $\beta$ -gal,  $1.8 \pm 0.5$  pA;  $p < 0.001$ ), but did not significantly alter the amplitude of NMDA-receptor-mediated currents in the same neurons (CPG15,  $3.9 \pm 0.6$  pA;  $\beta$ -gal,  $2.1 \pm 0.5$  pA; Fig. 5). CPG15 expression did not change the amplitudes of the AMPA- or NMDA-receptor-mediated currents in rostral tectal neurons (Fig. 5). In addition, the decrease in AMPA/NMDA ratio by tCPG15 in rostral cells was due to a selective reduction in the amplitude of AMPA-receptor-mediated currents (tCPG15,  $2.7 \pm 0.5$  pA;  $\beta$ -gal,  $4.8 \pm 0.8$  pA;  $p < 0.05$ ).

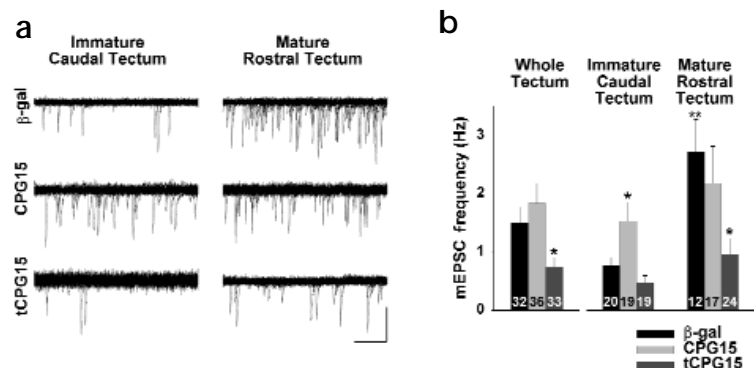
We have reported that the effect of CPG15 expression on tectal cell dendritic arbor growth is not cell autonomous<sup>24</sup>. To test whether the effect of CPG15 on synapse maturation is also not cell autonomous, we infected animals with a virus coexpressing a  $\beta$ -gal-GFP fusion protein along with CPG15, allowing ready identification of infected and uninfected tectal neurons during whole-cell

recordings. We recorded from 10 uninfected neurons in caudal tectum that were located close to infected GFP-expressing neurons. The average AMPA/NMDA ratio of these neurons was  $2.0 \pm 0.3$ . This value was significantly greater than the AMPA/NMDA ratio of control caudal neurons ( $0.9 \pm 0.1$ ), and is comparable to the AMPA/NMDA ratio of the pooled data of both infected and uninfected neurons ( $2.2 \pm 0.4$ ). These data clearly indicated that CPG15 affected synapse maturation in a non-cell-autonomous fashion. We did not specifically target infected neurons for recording. If infected neurons display an increase in synapse maturation, it could either be due to a cell-autonomous effect of CPG15 expression in that same neuron, or a non-cell-autonomous effect of CPG15 expression in another infected neuron.

As reflected in axonal and dendritic arbor growth, the effects of CPG15 on synaptic maturation required the GPI linkage to the cell membrane. Expression of tCPG15 significantly decreased AMPA/NMDA ratios at retinotectal synapses (Fig. 5), consistent with the decreased growth of tectal cell dendrites in animals expressing tCPG15-VV<sup>24</sup>. The effect of tCPG15 on AMPA/NMDA ratios was selective for neurons in rostral tectum (tCPG15,  $1.2 \pm 0.3$ ;  $\beta$ -gal,  $2.08 \pm 0.03$ ,  $p < 0.05$ ). Therefore, expression of tCPG15 caused neurons in mature tectal positions to have synaptic phenotypes characteristic of immature synapses (Fig. 5a and b).

NMDA receptor blockade severely attenuates dendritic arbor growth in simple tectal cells, in which NMDA-receptor-mediated current constitutes a significant portion of excitatory synaptic drive<sup>14</sup>. Furthermore, NMDA receptors are thought to be required for the addition of AMPA receptors to developing synapses<sup>7,33,34</sup>. To determine whether the effects of CPG15 expres-

**Fig. 7.** CPG15 increases the number of functional retinotectal synapses. (a) Examples of mEPSCs recorded from caudal and rostral neurons from brains infected with  $\beta$ -gal-, CPG15- and tCPG15-VV. Each panel is an overlay of 20 consecutive traces. CPG15 increased mEPSC frequency in caudal neurons, and tCPG15 decreased mEPSC frequency in rostral neurons. (b) mEPSC frequency averaged from all tectal cells recorded or separately for neurons from caudal and rostral tectum. CPG15 increased AMPA mEPSC frequency in caudal neurons. tCPG15 reduced AMPA mEPSC frequency in rostral and caudal neurons. The number of neurons analyzed are shown at the bottom of each bar. \*significant differences compared to relevant  $\beta$ -gal-VV controls,  $p < 0.05$ . \*\*significant differences between caudal and rostral neurons from animals infected with  $\beta$ -gal-VV.  $p < 0.05$ . Scale bar, 20 pA, 100 ms.



sion on synaptic maturation occur independently of NMDA receptor activity, we recorded from caudal tectal neurons in CPG15-expressing animals exposed to NMDA receptor antagonists throughout the period of viral expression of CPG15. These neurons show an increase in AMPA/NMDA ratio in response to CPG15 expression. Exposure to 50  $\mu$ M D-APV did not prevent the increase in AMPA/NMDA ratio seen with CPG15 expression (CPG15,  $2.2 \pm 0.4$ ; CPG15 + APV,  $2.3 \pm 0.3$ , Fig. 5d). These data indicate that CPG15 acts downstream of synaptic NMDA receptor activity to increase AMPA receptor insertion into synapses.

### CPG15 converts silent synapses to functional synapses

We used an analysis of failure rates of synaptic transmission to examine the effect of CPG15 on pre- and postsynaptic mechanisms regulating synaptic transmission. When recording under minimal stimulation conditions, a certain fraction of the afferent stimulation events fail to evoke a postsynaptic response. Responses recorded at depolarizing potentials detect both immature synapses with only NMDA receptors (silent synapses) and mature synapses with both NMDA and AMPA receptors. Mature synapses containing AMPA receptors are detected at hyperpolarizing potentials. Therefore, a cell with greater failure rates recorded at hyperpolarized potentials compared to depolarized potentials has immature synapses mediated solely by NMDA receptors. A selective decrease in failure rates recorded at hyperpolarizing potentials may reflect the insertion of AMPA receptors at silent synapses<sup>5,7,35</sup>. A change in failure rates recorded at both depolarized and hyperpolarized potentials may reflect a change in the probability of transmitter release at all glutamatergic synapses.

The fraction of synapses mediated solely by NMDA receptors decreases as neurons mature (caudal neurons,  $68.7 \pm 5.9\%$ ; rostral neurons,  $45.1 \pm 6.0\%$ ;  $p < 0.01$ ; Fig. 6). In optic tectal neurons from control  $\beta$ -gal-VV infected animals, the failure rates recorded at  $V_h = -60$  mV are relatively high in immature neurons from caudal tectum ( $70.8 \pm 5.8\%$ ) and decrease significantly in more mature rostral neurons ( $39.1 \pm 5.1\%$ ,  $p < 0.01$ ). This decrease occurs without a concomitant change in failure rates at  $V_h = +55$  mV (caudal,  $45.2 \pm 5.2\%$ ; rostral,  $31.2 \pm 6.2\%$ ), suggesting no significant change in probability of release.

CPG15 expression significantly decreased the fraction of silent synapses in the pooled sample of neurons recorded from the rostrocaudal extent of tectum (CPG15,  $40.3 \pm 7.4\%$ ;  $\beta$ -gal,  $60.8 \pm 5.9\%$ ;  $p < 0.05$ ). A separate analysis of failure rates in immature caudal neurons and mature rostral neurons indicated that CPG15 expression significantly reduced the fraction of silent synapses in caudal neurons compared to controls (CPG15,  $46.4 \pm 8.8\%$ ;  $\beta$ -gal,  $68.7 \pm 5.9\%$ ;  $p < 0.05$ ), but did not affect the rate of failures or fraction of silent synapses in mature rostral neurons. CPG15 expression decreased the failure rates recorded at  $V_h = -60$  mV from immature caudal neurons (CPG15,  $44.3 \pm 7.4\%$ ;  $\beta$ -gal,  $70.8 \pm 5.9\%$ ;  $p < 0.05$ ), but did not change failures at  $V_h = +55$  mV (CPG15,  $45.2 \pm 6.1\%$ ;  $\beta$ -gal,  $45.2 \pm 5.2\%$ ).

Conversely, tCPG15 expression significantly increased the estimated fraction of silent synapses in mature rostral neurons (tCPG15,  $66.8 \pm 8.0\%$ ;  $\beta$ -gal,  $45.1 \pm 6.0\%$ ;  $p < 0.05$ ; Fig. 6). Failure rates recorded at  $V_h = -60$  mV in mature rostral neurons were significantly greater in neurons from tCPG15-VV infected animals (tCPG15,  $64.6 \pm 7.5$ ;  $\beta$ -gal,  $39.1 \pm 5.1\%$ ;  $p < 0.05$ ), but failure rates at  $V_h = +55$  mV were not significantly altered (tCPG15,  $43.4 \pm 5.8\%$ ;  $\beta$ -gal,  $31.2 \pm 6.2\%$ ).

The decrease in silent synapses and increase in AMPA/NMDA ratios by CPG15 predicts that CPG15 expression will increase in

the number of synapses containing AMPA receptors. Such a change can be measured as a change in the frequency of spontaneous miniature EPSCs (mEPSCs) recorded at  $V_h = -60$  mV. In control neurons, the AMPA mEPSC frequency increases with neuronal maturation (Fig. 7). CPG15 expression increased the frequency of AMPA-receptor-mediated mEPSCs selectively in immature caudal neurons (CPG15,  $1.5 \pm 0.3$  Hz;  $\beta$ -gal,  $0.8 \pm 0.1$  Hz;  $p < 0.05$ ), without changing the amplitude of AMPA mEPSCs (data not shown).

Expression of tCPG15 significantly reduced AMPA mEPSC frequency in the pooled sample of all neurons recorded (Fig. 7). tCPG15 selectively decreased the AMPA mEPSC frequency in mature rostral neurons (tCPG15,  $1.0 \pm 0.3$  Hz;  $\beta$ -gal,  $2.7 \pm 0.6$ ;  $p < 0.01$ ) without reducing mEPSC frequency in caudal neurons. Furthermore, the AMPA receptor mEPSC frequency in mature rostral neurons from tCPG15 animals was similar to the mEPSC frequency in control immature neurons ( $0.8 \pm 0.1$  Hz). Therefore tCPG15 prevents the normal developmental increase in the number of synapses with functional AMPA receptors.

These results demonstrate that CPG15 promotes both synaptic maturation and morphological growth in the retinotectal system *in vivo* in a non-cell autonomous fashion. The three parameters we measured—the fraction of pure NMDA-receptor-mediated synapses, the AMPA/NMDA ratio and the frequency of AMPA mEPSCs—all indicate that CPG15 increases the incorporation of functional AMPA receptors into synapses. They further suggest that tCPG15 blocks or reverses the maturation of glutamatergic synapses.

### DISCUSSION

Brain development is characterized by a period of axonal and dendritic arbor growth and synaptogenesis. During this period, the elaboration of neuronal morphology and the formation of synaptic connections are intimately entwined. These observations suggest the existence of mechanisms that might coordinate several aspects of circuit formation. One potential scenario for the coordinated development of pre- and postsynaptic neuronal structures and synaptic connections within a circuit is as follows. Newly extended branches on axons and dendrites form synapses with only NMDA receptors. As these synapses mature, AMPA receptors are recruited to the synaptic sites. Mature AMPA-receptor-containing synapses stabilize the branches on which the synapses are located. Stabilized branches can then support the addition of new branches. These branches in turn establish new NMDA-receptor-only synapses, which are either stabilized through the addition of AMPA receptors or retracted. In control animals, as both tectal cell dendrites and RGC axons become more complex, the lifetime and stability of the arbor branches are determined by the strength of the synapses they make—branches that have established mature synaptic contacts remain, whereas those that fail to add AMPA receptors retract. In this way, during the growth phase of the circuit, the overall number of synaptic contacts is increased, as is the complexity of both axons and dendrites.

We propose that CPG15 expression in tectal neurons increases the elaboration of tectal cell dendrites and retinal axons through the same sequence of events including branch initiation, synapse formation, synapse maturation and branch stabilization. The increased retinal axon arbor growth rate is accomplished by a significant and selective decrease in axon branch retractions. Therefore, a major mechanism of regulating arbor elaboration is through the stabilization of newly added branches. Correlated with the stabilization of axonal branches is an increase in the strength of retinotectal synaptic transmission following CPG15 expression. This suggests that the strengthening of synaptic contacts between axon-

al and dendritic branches stabilizes the axon arbor branches. Therefore the increased dendritic and axonal growth rates occur together with the increased number of mature synapses.

CPG15 expression in tectal cells enhances retinal axon arbor growth, tectal cell dendritic arbor growth and retinotectal synapse formation, all in a non-cell-autonomous fashion. The primary site(s) of action of CPG15 is not yet known. In principle, there are three possibilities. One is that CPG15 could act on retinal axons, for instance to stabilize axonal branches. The changes in tectal cell morphology and synaptic physiology would then be secondary to the enhanced stability of presynaptic axons. CPG15 could also act on tectal cells. In this scenario, CPG15 expression in a tectal cell could trigger a 'maturation program' in neighboring tectal neurons, which would then feed back to presynaptic axons to enhance their branch stability and consequently, their growth rates. The CPG15-induced maturation program would cause the tectal cell to elaborate a complex dendritic arbor and add AMPA receptors to synapses. Our data support this hypothesis. The ability of CPG15 to increase AMPA/NMDA ratios in the presence of APV suggests that CPG15 may have a direct effect on dendrites independent of synaptically activated NMDA receptor activity. Furthermore, the changes in synaptic parameters that we have measured (increased AMPA/NMDA ratio, decreased failure rate, increased mEPSC frequency) are all consistent with a postsynaptic site of action of CPG15. A presynaptic site of action of CPG15 might be predicted to cause an increase in transmitter release, which would be detected as an increase in the amplitudes of both AMPA- and NMDA-receptor-mediated currents and an increase in AMPA mEPSC amplitude. A third possibility is that CPG15 could affect retinal axons and tectal cells independently of one another.

The maturation of synapses and their maintenance may operate through the regulation of AMPA receptor insertion and removal from the synaptic membrane<sup>36,37</sup>. CPG15 expression promotes synaptic maturation by increasing the AMPA/NMDA ratio and by decreasing the fraction of silent, NMDA-receptor-only retinotectal synapses. Furthermore, CPG15 increases the frequency but not the amplitude of AMPA-receptor-mediated mEPSCs. These data indicate that CPG15 enhances the maturation of retinotectal synapses by promoting the insertion of functional AMPA receptors into synapses previously mediated solely by NMDA receptors<sup>38</sup>.

Analysis of expression of tCPG15 indicates that CPG15 functions both to promote synapse maturation and to maintain established synapses. tCPG15 may block the normal maturation of retinotectal synapses by preventing the delivery of functional AMPA receptors to synapses. This interpretation is consistent with the decreased AMPA/NMDA ratios and increased fraction of pure NMDA receptor synapses in mature neurons, as well as the decreased mEPSC frequency seen with tCPG15 expression. The increased fraction of NMDA-receptor-only synapses in mature tectal neurons seen with tCPG15 is probably due to loss of AMPA receptors from synapses<sup>36</sup>. The increase in pure NMDA receptor synapses may in turn lead to retraction of branches bearing the silent synapses, accounting for the reduced dendritic arbor complexity detectable over longer time periods in neurons from animals expressing tCPG15 (ref. 24).

*In vivo* time-lapse imaging studies demonstrate that both axonal and dendritic growth are characterized by an early phase of rapid arbor growth, during which growth-promoting mechanisms predominate, followed by a later phase of slower growth, during which stop-growing mechanisms predominate. Our data suggest that these phases of neuronal development are controlled by temporally distinct activity-dependent mechanisms. The ini-

tial phase of rapid dendritic arbor growth occurs when glutamatergic synaptic input to the cell is dominated by NMDA receptors. The rapid growth is blocked selectively by exposure to NMDA receptor antagonists<sup>14</sup> and enhanced by CPG15 (ref. 24). A second activity-dependent mechanism that requires postsynaptic CaMKII normally restricts axonal and dendritic growth in complex arbors<sup>12,16</sup>. Postsynaptic expression of CPG15 enhances growth rates of complex presynaptic axons by maintaining them in a fast-growing and dynamic growth state, characteristic of simple axons. Viral expression of CPG15 seems to over-ride the endogenous mechanisms that normally restrict growth of complex retinal axons and tectal cell dendrites, consistent with the observation that NMDA receptor blockade did not inhibit CPG15-induced synaptic maturation.

Expression of *cpg15* in cultured cortical neurons can be induced through at least two different signaling pathways, one involving activation by BDNF and trkB receptors and a second involving membrane depolarization, voltage-dependent calcium channels and CaMKII<sup>18</sup>. BDNF promotes the elaboration of retinotectal axons in *Xenopus*<sup>39</sup>, and affects dendritic arbor elaboration<sup>40,41</sup> in an activity-dependent manner<sup>40</sup>, as well as affecting synaptic connectivity<sup>42</sup>. Therefore, the growth-promoting effect of BDNF and other neurotrophins might be mediated, at least in part, by CPG15.

CPG15 function requires its membrane attachment, as truncation of the GPI domain eliminates its ability to promote growth and synaptic maturation. The GPI anchor may permit CPG15 to cluster into rafts and associate with other components of a signaling complex<sup>22,23</sup>. Furthermore, given the potential for bi-directional signaling of GPI-linked proteins<sup>43</sup>, CPG15 may coordinate axo-dendritic growth and synaptic maturation by such a mechanism. Although many GPI-linked proteins function in axonal growth, including the ephrins<sup>22</sup>, semaphorins, fasciclin I, contactin, TAG1, NCAM and T-cadherin<sup>43,44</sup>, ephrin A5 (ref. 45) and NCAM<sup>46</sup> are also involved in synaptic plasticity, suggesting that proteins traditionally thought to function during axon guidance may have additional roles in circuit formation and plasticity.

## METHODS

**Imaging.** Retinal axons in anesthetized stage 42 albino *Xenopus laevis* tadpoles were labeled with DiI (1, 1'-diiodo-3,3',3',3'-tetramethylindocarbocyanine, DiI<sub>18</sub>(3); Molecular Probes, Eugene, Oregon) by iontophoresis, and imaged using a laser scanning confocal microscope (Noran Instruments, Madison, Wisconsin). Images were collected at 2 μm intervals with a 40 × oil lens (NA 1.30) as described<sup>47</sup>. Axons were imaged over a 2-day period to assess the effect of CPG15 expression on axon arbor growth rate. To assess arbor dynamics, images were collected every 2 h over an 8 h period. Tadpoles were individually housed in Steinberg's solution and kept at 25°C in a regulated 12 h red light/dark cycle.

**Viral infection.** Recombinant vaccinia virus expressed either CPG15, or a soluble form of CPG15 lacking the GPI consensus sequence (tCPG15)<sup>24</sup>. All viruses also expressed the reporter β-gal. Some electrophysiology experiments were performed with a virus expressing β-gal-EGFP fusion protein as a reporter. Genes of interest were driven by a strong synthetic early/late vaccinia virus promoter, and the reporter was driven by a weak p7.5 promoter<sup>48</sup>. Viruses were coded before infection for all experiments. Intraventricular virus injection and all subsequent data acquisition and analysis were performed blind to the virus code. Tectal cell infection with β-gal-VV has no effect on either presynaptic RGC axonal growth or dynamics, nor on synaptic responses, compared to uninfected animals<sup>5,12,15</sup>. The extent of virus infection was determined by β-gal immunohistochemistry<sup>24</sup>, or by EGFP imaging.

**Axon measurement.** Quantitation and analysis of axonal branch length and branch number were performed as described previously<sup>15</sup>. Analysis of branch dynamics was performed as described<sup>28</sup>. Axons were categorized as simple or complex according to the total axonal branch length measurements on day 0, before virus injection. Statistical significance was determined using Student's *t*-tests.

**Electrophysiology.** Electrophysiological recordings were performed at room temperature on an isolated whole-brain preparation described<sup>5</sup>, 2–3 days after viral infection. Neurons had input resistances in the range of 1 to 4 gigaohm and series resistance of less than 50 megaohm, which were monitored throughout each experiment. We quantified the amplitude of NMDA- and AMPA-receptor-mediated currents and the fraction of silent synapses as described<sup>5</sup>. AMPA-receptor-mediated mEPSCs were recorded at  $V_h = -60$  mV with tetrodotoxin (1  $\mu$ M) in the bath solution. The mEPSCs were analyzed with Mini Analysis Program (Jaegin Software, Leonia, New Jersey). Neurons were grouped according to their location in the caudal or rostral half of the tectum. Viruses were coded before injection, and all recordings and analysis were done blind to viral type.

To test the role of NMDA receptors in CPG15 function, we added 5-aminophosphonovalerate (D-APV, 50  $\mu$ M) to the rearing solution immediately after ventricular injection of either  $\beta$ -gal- or CPG15-VV. Fresh APV solution was exchanged every 12 h. Bath application of APV reduced tadpole mobility, indicating that it penetrated the CNS.

#### ACKNOWLEDGEMENTS

We thank Elly Nedivi for generating the recombinant CPG15 and tCPG15 viruses, Kim Bronson for technical assistance, Dominik Rosa and David Beck for help with data analysis, and Dong-Jing Zou for help with axonal labeling. We also thank Zach Mainen and Josh Huang and members of the Cline lab for comments on the manuscript. This work was supported by the Ministerio de Educación y Ciencia from Spain (I.C.), an NEI NRSA (K.H.) and the NEI (H.T.C.).

RECEIVED 1 MAY; ACCEPTED 15 AUGUST 2000

1. Antonini, A. & Stryker, M. P. Rapid remodeling of axonal arbors in the visual cortex. *Science* **260**, 1819–1821 (1993).
2. Mainen, Z. F. & Sejnowski, T. J. Influence of dendritic structure on firing pattern in model neocortical neurons. *Nature* **382**, 363–366 (1996).
3. Fiala, J. C. & Harris, K. M. in *Dendrites* (eds. Stuart, G., Spruston, N. & Häusser, M.) 1–34 (Oxford Univ. Press, New York, 1999).
4. Spruston, N., Stuart, G. & Häusser, M. in *Dendrites* (eds. Stuart, G., Spruston, N. & Häusser, M.) 231–270 (Oxford Univ. Press, New York, 1999).
5. Wu, G., Malinow, R. & Cline, H. T. Maturation of a central glutamatergic synapse. *Science* **274**, 972–976 (1996).
6. Li, P. & Zhuo, M. Silent glutamatergic synapses and nociception in mammalian spinal cord. *Nature* **393**, 695–698 (1998).
7. Liao, D. & Malinow, R. Deficiency in induction but not expression of LTP in hippocampal slices from young rats. *Learn. Mem.* **3**, 138–149 (1996).
8. Isaac, J. T. R., Crair, M. C., Nicoll, R. A. & Malenka, R. C. Silent synapses during development of thalamocortical inputs. *Neuron* **18**, 1–20 (1997).
9. Feldman, D. E., Brainard, M. S. & Knudsen, E. I. Newly learned auditory responses mediated by NMDA receptors in the owl inferior colliculus. *Science* **271**, 525–528 (1996).
10. Nusser, Z. *et al.* Cell type and pathway dependence of synaptic AMPA receptor number and variability in the hippocampus. *Neuron* **21**, 545–559 (1998).
11. Petralia, R. S. *et al.* Selective acquisition of AMPA receptors over postnatal development suggests a molecular basis for silent synapses. *Nat. Neurosci.* **2**, 31–36 (1999).
12. Wu, G. Y. & Cline, H. T. Stabilization of dendritic arbor structure in vivo by CaMKII. *Science* **279**, 222–226 (1998).
13. Wu, G. Y., Zou, D. J., Rajan, I. & Cline, H. T. Dendritic dynamics in vivo change during neuronal maturation. *J. Neurosci.* **19**, 4472–4483 (1999).
14. Rajan, I. & Cline, H. T. Glutamate receptor activity is required for normal development of tectal cell dendrites in vivo. *J. Neurosci.* **18**, 7836–7846 (1998).
15. Zou, D. J. & Cline, H. T. Expression of constitutively active CaMKII in target tissue modifies presynaptic axon arbor growth. *Neuron* **16**, 529–539 (1996).
16. Zou, D. J. & Cline, H. T. Postsynaptic calcium/calmodulin-dependent protein kinase II is required to limit elaboration of presynaptic and postsynaptic neuronal arbors. *J. Neurosci.* **19**, 8909–8918 (1999).
17. Nedivi, E. Molecular analysis of developmental plasticity in neocortex. *J. Neurobiol.* **41**, 135–147 (1999).
18. Naeve, G. S. *et al.* Neuritin: a gene induced by neural activity and

- neurotrophins that promotes neuritogenesis. *Proc. Natl. Acad. Sci. USA* **94**, 2648–2653 (1997).
19. Nedivi, E., Hevroni, D., Naot, D., Israeli, D. & Citri, Y. Numerous candidate plasticity-related genes revealed by differential cDNA cloning. *Nature* **363**, 718–722 (1993).
20. Nedivi, E., Fieldust, S., Theill, L. E. & Hevron, D. A set of genes expressed in response to light in the adult cerebral cortex and regulated during development. *Proc. Natl. Acad. Sci. USA* **93**, 2048–2053 (1996).
21. Corriveau, R. A., Shatz, C. J. & Nedivi, E. Dynamic regulation of cpG15 during activity-dependent synaptic development in the mammalian visual system. *J. Neurosci.* **19**, 7999–8008 (1999).
22. Flanagan, J. G. & Vanderhaeghen, P. The ephrins and Eph receptors in neural development. *Annu. Rev. Neurosci.* **21**, 309–345 (1998).
23. Horejsi, V. *et al.* GPI-microdomains: a role in signaling via immunoreceptors. *Immunol. Today* **20**, 356–361 (1999).
24. Nedivi, E., Wu, G. Y. & Cline, H. T. Promotion of dendritic growth by CPG15, an activity-induced signaling molecule. *Science* **281**, 1863–1866 (1998).
25. Sakaguchi, D. S. & Murphey, R. K. Map formation in the developing *Xenopus* retinotectal system: an examination of ganglion cell terminal arborizations. *J. Neurosci.* **5**, 3228–3245 (1985).
26. Fujisawa, H. Mode of growth of retinal axons within the tectum of *Xenopus* tadpoles, and implications in the ordered neuronal connection between the retina and the tectum. *J. Comp. Neurol.* **260**, 127–139 (1987).
27. O'Rourke, N. A. & Fraser, S. E. Dynamic changes in optic fiber terminal arbors lead to retinotopic map formation: an *in vivo* confocal microscopic study. *Neuron* **5**, 159–171 (1990).
28. Witte, S., Stier, H. & Cline, H. T. *In vivo* observations of timecourse and distribution of morphological dynamics in *Xenopus* retinotectal axon arbors. *J. Neurobiol.* **31**, 219–234 (1996).
29. Hickmott, P. W. & Constantine-Paton, M. The contributions of NMDA, non-NMDA and GABA receptors to postsynaptic responses in neurons of the optic tectum. *J. Neurosci.* **13**, 4339–4353 (1993).
30. Zhang, L. L., Tao, H. W., Holt, C. E., Harris, W. A. & Poo, M.-M. A critical window for cooperation and competition among developing retinotectal synapses. *Nature* **395**, 37–44 (1998).
31. Gaze, R. M., Keating, M. J., Ostberg, A. & Chung, S. H. The relationship between retinal and tectal growth in larval *Xenopus*: Implications for the development of the retinotectal projection. *J. Embryol. Exp. Morph.* **53**, 103–143 (1979).
32. Reh, T. & Constantine-Paton, M. Retinal ganglion cells change their projection sites during larval development of *Rana pipiens*. *J. Neurosci.* **4**, 442–457 (1984).
33. Durand, G. M., Kovalchuk, Y. & Konnerth, A. Long-term potentiation and functional synapse induction in developing hippocampus. *Nature* **381**, 71–75 (1996).
34. Zhang, L. L., Toa, H.-z. W. & Poo, M.-M. Visual input induces long-term potentiation of developing retinotectal synapses. *Nat. Neurosci.* **3**, 708–715 (2000).
35. Malinow, R. Transmission between pairs of hippocampal slice neurons: quantal levels, oscillations, and LTP. *Science* **252**, 722–724 (1991).
36. Carroll, R. C., Lissin, D. V., von Zastrow, M., Nicoll, R. A. & Malenka, R. C. Rapid redistribution of glutamate receptors contributes to long-term depression in hippocampal cultures. *Nat. Neurosci.* **2**, 454–460 (1999).
37. Hayashi, Y. *et al.* Driving AMPA receptors into synapses by LTP and CaMKII: requirement for GluR1 and PDZ domain interaction. *Science* **287**, 2262–2267 (2000).
38. Shi, S. H. *et al.* Rapid spine delivery and redistribution of AMPA receptors after synaptic NMDA receptor activation. *Science* **284**, 1811–1816 (1999).
39. Cohen-Cory, S. & Fraser, S. E. Effects of brain-derived neurotrophic factor on optic axon branching and remodelling in vivo. *Nature* **378**, 192–196 (1995).
40. McAllister, A. K., Katz, L. C. & Lo, D. C. Neurotrophin regulation of cortical dendritic growth requires activity. *Neuron* **17**, 1057–1064 (1996).
41. Yacoubian, T. A. & Lo, D. C. Truncated and full-length TrkB receptors regulate distinct modes of dendritic growth. *Nat. Neurosci.* **3**, 342–349 (2000).
42. Jankowsky, J. L. & Patterson, P. H. Cytokine and growth factor involvement in long-term potentiation. *Mol. Cell Neurosci.* **14**, 273–286 (1999).
43. Faivre-Sarrailh, C. & Rougon, G. Axonal molecules of the immunoglobulin superfamily bearing a GPI anchor: their role in controlling neurite outgrowth. *Mol. Cell Neurosci.* **9**, 109–115 (1997).
44. Walsh, F. S. & Doherty, P. Glycosylphosphatidylinositol anchored recognition molecules that function in axonal fasciculation, growth and guidance in the nervous system. *Cell Biol. Int. Rep.* **15**, 1151–1166 (1991).
45. Gao, W. Q. *et al.* Regulation of hippocampal synaptic plasticity by the tyrosine kinase receptor, REK7/EphA5, and its ligand, AL-1/Ephrin-A5. *Mol. Cell Neurosci.* **11**, 247–259 (1998).
46. Cremer, H. *et al.* Long-term but not short-term plasticity at mossy fiber synapses is impaired in neural cell adhesion molecule-deficient mice. *Proc. Natl. Acad. Sci. USA* **95**, 13242–13247 (1998).
47. Cline, H. T., Edwards, J. A., Rajan, I., Wu, G. Y. & Zou, D. J. in *Imaging: A Laboratory Manual* (eds. Yuste, R., Lanni, F. & Konnerth, A.) 13.1–13.12 (Cold Spring Harbor Laboratory Press, Cold Spring Harbor, New York, 1999).
48. Wu, G. Y., Zou, D. J., Koothan, T. & Cline, H. T. Infection of frog neurons with vaccinia virus permits *in vivo* expression of foreign proteins. *Neuron* **14**, 681–684 (1995).